

1    Population genetic inferences using immune gene SNPs mirror  
2                                    patterns inferred by microsatellites

3                                    JEAN P. ELBERS<sup>1,3</sup>, RACHEL W. CLOSTIO<sup>2</sup>, SABRINA S. TAYLOR<sup>1</sup>

<sup>1</sup>School of Renewable Natural Resources, 227 RNR Bldg., Louisiana State University and AgCenter,  
Baton Rouge, Louisiana, 70803, USA

<sup>2</sup>Department of Biology, 300 E. St. Mary Blvd., University of Louisiana at Lafayette,  
Lafayette, Louisiana, 70503, USA

Keywords: microsatellites, target enrichment, sequence capture,  
next-generation sequencing, immunogenetics, population genomics

<sup>3</sup>Corresponding author: Fax: 225-578-4227, Email: [jean.elbers@gmail.com](mailto:jean.elbers@gmail.com)

Running title: Immune gene SNPs mirror microsatellites

## Abstract

Single nucleotide polymorphisms (SNPs) are replacing microsatellites for population genetic analyses, but it is not apparent how many SNPs are needed or how well SNPs correlate with microsatellites. We used data from the gopher tortoise, *Gopherus polyphemus* - a species with small populations, to compare SNPs and microsatellites to estimate population genetic parameters. Specifically, we compared one SNP dataset (16 tortoises from 4 populations sequenced at 17,901 SNPs) to two microsatellite datasets, a full dataset of 101 tortoises and a partial dataset of 16 tortoises previously genotyped at 10 microsatellites. For the full microsatellite dataset, observed heterozygosity, expected heterozygosity, and  $F_{ST}$  were correlated between SNPs and microsatellites; however, allelic richness was not. The same was true for the partial microsatellite dataset, except that allelic richness, but not observed heterozygosity, was correlated. The number of clusters estimated by Structure differed for each dataset (SNPs = 2; partial microsatellite = 3; full microsatellite = 4). PCA showed four clusters for all datasets. More than 800 SNPs were needed to correlate with allelic richness, observed heterozygosity, and expected heterozygosity, but only 100 were needed for  $F_{ST}$ . The number of SNPs typically obtained from NGS far exceeds the number needed to correlate with microsatellite parameter estimates. Our study illustrates that diversity,  $F_{ST}$ , and PCA results from microsatellites can mirror those obtained with SNPs. These results may be generally applicable to small populations, a defining feature of endangered and threatened species, because theory predicts that genetic drift will tend to outweigh selection in small populations.

## Introduction

Molecular markers vary in their utility and application to population genetic studies, and geneticists use available markers suited to answering questions at hand. Initially, geneticists only had allozymes and used them to infer nucleotide changes underlying differences in protein migration during electrophoresis. Later, variable mitochondrial DNA markers were used because of the availability of conserved primers and the high copy number of mitochondria, but mitochondrial markers mostly provided information on broad-scale genetic patterns (Moritz, 1994). Presently, markers such as microsatellites are commonly used in population genetics because most are presumed neutral, are found throughout genomes, and can elucidate fine-scale spatial genetic patterns (e.g., Clostio *et al.*, 2012).

Genomic resources, hybridization arrays, fluorescent probes, and next-generation sequencing (NGS) have allowed researchers to access other types of genomic markers, and recently large arrays of single nucleotide

polymorphisms (SNPs) have become particularly popular in population genetic studies of not only model but also non-model organisms (Allendorf *et al.*, 2010). SNPs are one of the most numerous molecular markers (Gupta *et al.*, 2001), and thousands to millions of them can be examined simultaneously using NGS techniques compared to dozens observed in traditional Sanger sequencing-based approaches. However, as the preferred tool shifts from microsatellites to genome-wide SNPs, it is important to understand new results in the context of previous research.

Prior research has shown that microsatellite-derived population genetic parameters generally correlate with parameters derived SNPs. Most data from pre-NGS SNP methods find correlations between microsatellites and SNPs (e.g., Ryynanen *et al.*, 2007; Narum *et al.*, 2008; Coates *et al.*, 2009; Glover *et al.*, 2010; Garke *et al.*, 2012), but there are some exceptions (e.g., Vali *et al.*, 2008; DeFaveri *et al.*, 2013). Considerably fewer studies have compared genetic inferences derived from microsatellites to inferences from thousands of NGS generated SNPs, but there are some examples from restriction site-associated DNA sequencing (RADseq) studies where correlations are present (Jeffries *et al.*, 2016) between the two types of markers for population genetic parameters or not (Lozier, 2014). As more and more studies use NGS data, a better understanding of this relationship is imperative because many current management and recovery plans currently in effect are based on genetic data from microsatellites, and these plans may change if results from microsatellites and NGS data are consistently and substantively different.

Microsatellites are presumed to be neutrally evolving and most likely influenced by neutral genetic processes while SNPs can be influenced by either neutral or adaptive genetic processes. SNPs can represent functional, coding regions of the genome, which on the one hand are under purifying selection to avoid deleterious changes and on the other under positive selection for advantageous changes. For example, SNPs present in genes that influence immune response are likely to be under strong positive selection as such changes could provide resilience to infectious disease (Bernatchez & Landry, 2003; Sommer, 2005).

Although genes such as immune genes are predicted to be under strong selective pressure, small effective population sizes ( $N_e$ ) can make genes influenced by selection behave like effectively neutral loci. In particular, loci under selection may be effectively neutral if their selection coefficient ( $s$ ) is less than or equal to  $(1/(2N_e))$  (Wright, 1931). For example, for alleles of immune response genes such as those of the major histocompatibility complex (MHC), which can have high selection coefficients of 1%, such alleles could behave like effectively neutral loci if effective population sizes are less than 50 individuals (Frankham *et al.*, 2010). Empirical studies support these conclusions as MHC loci behave like effectively neutral loci for a variety of threatened vertebrates with small, bottlenecked populations (Weber *et al.*, 2004; Miller *et al.*, 2008; Taylor

64 *et al.*, 2012).

65 We recently applied genomic approaches to the threatened (gopher tortoise) *Gopherus polyphemus* by iso-  
66 lating genes involved in immune responses to better understand susceptibility to a chronic and occasionally  
67 fatal infectious upper respiratory tract disease (Elbers & Taylor, 2015). These samples were also previously  
68 genotyped at 10 microsatellites by Clostio *et al.* (2012) providing an excellent opportunity to compare pop-  
69 ulation genetic parameters derived from presumably neutrally evolving microsatellites and presumably drift  
70 and/or selection-influenced immune gene SNPs from an organism with generally small population sizes.

71 We leveraged the NGS (Elbers & Taylor, 2015) and microsatellite (Clostio *et al.*, 2012) data already  
72 collected for *G. polyphemus* to compare estimates of population genetic diversity, differentiation, and admix-  
73 ture derived from immune gene SNPs and microsatellites using samples from the same populations to better  
74 understand how NGS SNP inferences relate to those from microsatellites. We also subsample our SNPs to  
75 determine how many are needed to replace a given number of microsatellites for estimating genetic diver-  
76 sity and differentiation. Although immune gene SNPs are putatively under selection and microsatellites are  
77 presumably neutral, we predict inferences from immune gene SNPs will mostly correlate with microsatellite  
78 inferences as there will be a preponderance of selectively neutral immune gene SNPs due to the generally  
79 small population sizes of *G. polyphemus*. We also predict that not all of the discovered SNPs will be needed  
80 to replace microsatellites for estimating diversity and differentiation.

## 81 Methods

### 82 Samples

83 Because SNP analyses are often costly, smaller sample sizes than those used in microsatellite studies are  
84 typical. In this study we were interested in how a smaller sample size but a larger number of SNP markers  
85 would compare to a typical microsatellite dataset. We were limited to analyzing SNPs from 16 tortoises,  
86 so we randomly chose 16 *G. polyphemus* from 4 sample populations (4 per population, Fig. 1). These 4  
87 sample populations were chosen out of the 24 used by Clostio *et al.* (2012) because they were distributed  
88 along an east to west gradient and were likely representative of the genetic variability for the species. We  
89 compared the SNP dataset to two microsatellite datasets: (1) the full microsatellite dataset of 101 tortoises  
90 sampled by Clostio *et al.* (2012) (Table 1); and, (2) a partial microsatellite dataset of 16 tortoises. We used  
91 two microsatellite datasets to: 1) equalize sample size (partial), and ; 2) use a sample size representative of a  
92 typical microsatellite study (full). Only 1 GA tortoise in the SNP dataset had been previously genotyped at

all 10 microsatellite loci by Clostio *et al.* (2012), so for the partial microsatellite dataset, we randomly chose 3 additional tortoises from the GA population that had been genotyped at all 10 microsatellites. Thus, the SNP dataset and the partial microsatellite dataset only differed by 3 samples from the GA population.

## Target region for sequencing SNPs

The methods for acquiring SNP data are presented in Elbers & Taylor (2015). Briefly, we created a target region to capture the immunome (i.e., genes involved in immune response, *sensu amplo* Ortutay & Vihinen (2006)) of *Chrysemys picta bellii* (western painted turtle) using the GO2TR workflow (Elbers & Taylor, 2015). The workflow filtered the *C. p. bellii* 3.0.1 genome assembly (Shaffer *et al.*, 2013) annotated by the NCBI Eukaryotic Genome Annotation Pipeline (annotation release 100) using the gene ontology term "immune response" (i.e., genes that function in the immune system's response to internal or invasive threats). Jean-Marie Rouillard of MYcroarray Inc. (Ann Arbor, MI, USA) generated 120-bp bait sequences with 60-bp overlap to capture our 1.4Mbp target region.

## Library preparation and sequence capture

We used biotinylated RNA baits from MYcroarray in an in-solution hybridization experiment to capture the immunomes of 16 *G. polyphemus*. We created 16 Illumina adaptor-ligated libraries using Agilent SureSelect XT2 Reagent Kits for the Illumina MiSeq (Agilent Technologies, Santa Clara, CA, USA), pooled 16 prepared libraries per capture reaction, and used MYcroarray reagents and protocols for sequence capture. We then sequenced post-capture amplification libraries on two Illumina MiSeq sequencer flow cells (i.e., all individuals sequenced twice) using MiSeq version 3 chemistry and 75-bp paired-end reads at Pennington Biomedical Research Center (Baton Rouge, LA, USA).

## Read quality control and mapping

We demultiplexed reads for each MiSeq run, allowing for up to one mismatch in the 8-bp barcode using MiSeq Reporter software. We used TRIMMOMATIC v0.32 (Bolger *et al.*, 2014) default settings for adapter trimming, and for base quality filtering, we trimmed leading and trailing bases with quality scores less than 5 and 15, respectively. We also used sliding window scans to remove the 3' end of reads when average quality dropped below 15, and discarded reads with less than 40 bases. We next merged overlapping paired-ends reads with BBMerge v5.4 from the BBMap suite (<https://sourceforge.net/projects/bbmap/>) and then combined unpaired single reads (n=9.08 million) and merged paired reads for downstream analysis. Paired

121 and single plus merged reads were first mapped separately to the *C. p. bellii* 3.0.3 genome using the BWA-MEM  
122 algorithm (Li, 2013) implemented in BWA v0.7.12 (Li & Durbin, 2009), and then less stringently using STAMPY  
123 v1.0.23 (Lunter & Goodson, 2011). We used SAMTOOLS v1.1 (Li *et al.*, 2009) to merge binary alignment map  
124 (BAM) files from paired reads and single plus merged reads. NCBI remap ([http://www.ncbi.nlm.nih.gov/  
125 genome/tools/remap](http://www.ncbi.nlm.nih.gov/genome/tools/remap)) was used to convert our bait intervals from *C. p. bellii* 3.0.1 to *C. p. bellii* 3.0.3  
126 coordinates.

## 127 **Variant and genotype calling**

128 Mapped reads were then processed using the Genome Analysis Toolkit v3.3.0 (McKenna *et al.*, 2010,  
129 GATK), adhering to GATK best practices for exome sequencing and calling variants such as SNPs with GATK's  
130 Haplotype Caller and Unified Genotyper.

131 We then filtered variants to remove those with bad validation, low quality, low read depth, or low genotype  
132 quality to produce a high quality set of SNPs called by the Unified Genotyper. Next, we called variants  
133 from base-recalibrated BAM files using the Haplotype Caller and filtered variants in the same manner  
134 as before. We then looked for concordance between the two variant callers and used concordant SNPs for  
135 variant quality filtering of the Haplotype Caller's call set. Finally, we used BEAGLE v4.0 r1398 (Browning  
136 & Browning, 2007) for genotype imputation on the variant-recalibrated SNP set. Following variant calling,  
137 we used PICARD's v1.128 (<http://broadinstitute.github.io/picard/>) CalculateHSMetrics to estimate  
138 sequencing metrics, and featureCounts (Liao *et al.*, 2014) to estimate the number of genes and exons covered  
139 by each sample.

## 140 **Population genomic analyses**

141 For all population genomic analyses, we analyzed only di-allelic polymorphic SNP loci, as the tri- (n=758)  
142 and tetra-allelic (n=7) loci we obtained would influence SNP heterozygosity estimates. We used VCFTTOOLS  
143 v0.1.12b (Danecek *et al.*, 2011) to recalculate allele frequencies from our Beagle-imputed SNPs and then  
144 removed loci with allele frequencies of one. We then pruned SNP loci that were out of Hardy-Weinberg  
145 Equilibrium (HWE) or in Linkage Disequilibrium (LD) within each population using default settings in  
146 VCFTTOOLS. We used the `p.adjust` function in R (R Core Team, 2015) to correct *P* values for HWE and LD  
147 tests using a false discovery rate (Benjamini & Hochberg, 1995) of 0.05.

148 We examined what polymorphic SNPs might be under selection with BayeScan v2.1 (Foll & Gag-  
149 giotti, 2008) with the intent of pruning those SNPs that were putatively under selection. We used the

150 `make_bayescan_input.py` script to convert variant call format (VCF) to **BayeScan** input format (De Wit  
151 *et al.*, 2012) and a false discovery rate of 0.05. In order for a given SNP to be included in the analysis, we  
152 required at least four good quality genotypes from each population and at least one copy of the minor allele  
153 for a locus.

154 For genetic diversity analyses and all subsequent file conversions, we used **PGDSpider** v2.0.7.4 (Lischer  
155 & Excoffier, 2012) and the R package **hierfstat** v0.04-10 (Goudet, 2005) to assess observed and expected  
156 heterozygosity and allelic richness. For population genomic differentiation, we estimated  $F_{ST}$  values with  
157 **hierfstat**. For estimating admixture, we performed principle component analyses (PCA) with **hierfstat**,  
158 and we also assessed population admixture using **STRUCTURE** v2.3.4 (Pritchard *et al.*, 2000; Hubisz *et al.*,  
159 2009). We ran **STRUCTURE** with 100,000 burnins and 1,000,000 replicates using correlated allele frequency and  
160 the admixture ancestry models from  $K=1-5$  with 20 replicates per  $K$  value. We used **STRUCTURE HARVESTER**  
161 web v0.6.94 (Earl & vonHoldt, 2012) to select the best  $K$  value and **CLUMPAK** web server (Kopelman *et al.*,  
162 2015) to average data from multiple runs and to visualize population assignments.

## 163 **Microsatellite analyses**

164 We assessed HWE and LD for the full and partial microsatellite datasets using **ARLEQUIN** v3.5 (Excoffier  
165 & Lischer, 2010). All 10 loci for both datasets were in HWE and linkage equilibrium. Genetic diversity,  
166 differentiation, and admixture were estimated in the same manner as SNPs using **hierfstat** and **STRUCTURE**.

## 167 **Random sampling of SNPs for subsampling analysis**

168 We examined how many SNP loci would be needed to obtain  $P$  values  $< 0.05$  for Pearson's  $r$  correlation  
169 coefficient with the full and partial microsatellite datasets for allelic richness, heterozygosities, and  $F_{ST}$  values  
170 by randomly subsampling our 17,901 SNPs. We did not include allelic richness when comparing the SNP and  
171 full microsatellite datasets because they were not correlated at the 0.05 level, and we did not include allelic  
172 richness and observed heterozygosity when comparing the SNP and partial microsatellite datasets because  
173 they were not correlated. We randomly chose SNPs among the following sample sizes using a custom R script:  
174 10, 20, 40, 100, 200, 400, 800, 1,600, 3,200, 6,400, or 13,200 SNPs and calculated the  $P$  value of the Pearson's  
175 correlation coefficient using the `cor.test` function in R for each sample size of SNP loci for allelic richness,  
176 observed heterozygosity, expected heterozygosity, and  $F_{ST}$ . We repeated the process and chose 10 replicates  
177 for each sample size for both the full and partial microsatellite datasets.

## Effective population size

We estimated effective population size using the full microsatellite and SNP datasets with the program `NeEstimator` v2.01 (Do *et al.*, 2014) and employed one single-sample estimator of  $N_e$  (i.e., the linkage disequilibrium method of Waples & Do (2008)), and two single-sample estimators of the number of effective breeders per year (i.e.,  $N_b$  using the heterozygote-excess method of Zhdanova & Pudovkin (2008) and the molecular coancestry method of Nomura (2008)). We converted  $N_b$  to  $N_e$  by multiplying  $N_b$  by the generation time of 31 years for the gopher tortoise (Enge *et al.*, 2006).

## Results

From two Illumina MiSeq sequencer runs, we obtained 47.5 million reads that passed quality control and were assignable to individuals. Each tortoise had  $3 \pm 0.7$  (mean  $\pm$  standard deviation) million reads of which  $47.9 \pm 3.2$  % were unique (i.e., were not PCR duplicates), and  $98.8 \pm 0.1$  % of these unique reads could be aligned to our target region (Table S1, Supporting information). Mean sample coverage over the entire target region was  $65.4 \pm 13$  reads, and each sample had  $69.3 \pm 3.6$  % target bases with coverage greater than 20 reads (Fig. S2, Fig. S3, Supporting information). Only 4.7 % (66.3 Kbp) of the 1.4 Mbp target region had coverage of less than 2 reads. Although our target region contained a total of 632 immune genes and 5,425 exons, only 611 genes and 4,837 exons were represented by usable reads. Each sample had reads for  $592.1 \pm 4.2$  genes and  $4,106 \pm 98.1$  exons (mean  $\pm$  standard deviation).

There were 17,901 di-allelic polymorphic SNP loci after filtering and imputation. None of these loci were out of HWE or in LD, but the lack of LD is unlikely given the close proximity of loci within the same exon. This may have occurred because we had to correct  $P$  values to account for thousands of multiple tests. Polymorphic SNPs were present in 491 immune genes (Table S2, Supporting information) and included broad classes such as major histocompatibility and Toll-like receptor genes (Table 2).

There were 66 SNP loci that may have been under selection, which represented 31 genes. Pruning these SNPs did not significantly influence results, so we chose to analyze the full SNP dataset when comparing genetic diversity, differentiation, or admixture between SNPs and microsatellites.

SNP allelic richness was not positively correlated with values derived from the full microsatellite dataset (Fig. 2A, Pearson's  $r = 0.411$ ,  $P = 0.294$ ); however, SNP and microsatellite observed (Fig. 2B, Pearson's  $r = 0.945$ ,  $P = 0.028$ ) and expected heterozygosities (Fig. 2C, Pearson's  $r = 0.976$ ,  $P = 0.012$ ) were highly correlated. Allelic richness was correlated between the SNP and partial microsatellite datasets (Fig. 2E,



207 Pearson's  $r = 0.992$ ,  $P = 0.004$ ). Observed heterozygosity was not correlated (Fig. 2F, Pearson's  $r = 0.63$ ,  
208  $P = 0.185$ ), but expected heterozygosity was (Fig. 2G, Pearson's  $r = 0.924$ ,  $P = 0.038$ ). The LA population  
209 followed by FL then GA and AL populations had the lowest to highest heterozygosity and allelic richness for  
210 SNPs. This suggests lower genetic diversity in the western LA population versus eastern FL, GA, and AL  
211 populations based on SNPs, a similar result to that obtained with both microsatellite datasets.

212 Pairwise  $F_{ST}$  values were also positively correlated for SNP and the full (Fig. 2D, Pearson's  $r = 0.96$ ,  $P$   
213  $= 0.001$ ) and partial (Fig. 2H, Pearson's  $r = 0.968$ ,  $P = 0.001$ ) microsatellite datasets. However, LA and  
214 AL had the lowest differentiation for SNPs compared to second lowest for microsatellites.

215 Population admixture inferred using SNPs suggested an optimum number of two clusters with **STRUCTURE**,  
216 the first consisting of AL, GA, and LA; the second with FL by itself (Fig. S3, Supporting information). For  
217 the full microsatellite dataset, there was an optimum of four clusters: one for each population examined (Fig.  
218 S4, Supporting information). The partial microsatellite dataset had three optimum clusters: the first with  
219 LA; the second with AL and GA; and the third with FL (Fig. S5, Supporting information). PCA analysis  
220 produced four clusters for SNPs and both microsatellite datasets (one for each population, Fig. 3A–3C).

221 Random sampling of SNP loci showed that at least 1,600 SNPs were needed to obtain a significant correla-  
222 tion between SNP- and the full microsatellite dataset for allelic richness (Fig. S6A, Supporting information).  
223 Nearly 800 SNPs were needed for expected heterozygosity (Fig. S6B, Supporting information), but only 100  
224 SNPs were needed for SNP- and microsatellite-derived  $F_{ST}$  values to be correlated (Fig. S6C). There was  
225 a similar pattern for the partial microsatellite dataset for allelic richness, expected heterozygosity, and  $F_{ST}$ ,  
226 where at least 800, 800, and 100 SNPs were needed for significant correlations, respectively (Fig. S7A–7C,  
227 Supporting information). Parameter variability decreased as the number of randomly chosen SNPs increased,  
228 especially after 200, 100, 40, and 40 SNPs for allelic richness, observed and expected heterozygosity, and  $F_{ST}$   
229 values respectively (Fig. S6, Fig. S7, Supporting information).

230 Effective population sizes estimated using the full microsatellite dataset were not particularly informative,  
231 especially the estimates of infinite population sizes from the heterozygous-excess and linkage disequilibrium  
232 methods (Fig. S8A, Supporting information). Minus the FL population's estimate of infinite effective pop-  
233 ulation size, the molecular coancestry method suggested more reasonable estimates of effective population  
234 sizes between 34–589 individuals per population. Effective population sizes estimated using immune gene  
235 SNPs were more realistic with the heterozygous-excess method suggesting between 133–186 tortoises, and the  
236 molecular coancestry method suggesting between 319–427 tortoises per population (Fig. S8B, Supporting  
237 information). The linkage disequilibrium method was not informative as all effective population sizes were

estimated to be infinite.

The  $N_e$  estimates that ranged between 34–589 individuals (microsatellite and SNP molecular coancestry and SNP heterozygous-excess approaches) suggest that selection coefficients for SNPs would need to be less than 0.1% for genetic drift to outweigh selection.

## Discussion

Estimates of genetic diversity derived from gopher tortoise immunome SNPs and both microsatellite datasets were typically correlated. Given that most gopher tortoise populations are small, immune gene SNPs may be behaving like effectively neutral loci. Thus, these correlations are theoretically reasonable and may hold true for other small populations, for example, endangered and threatened species generally.

Other studies have observed similar and contrasting correlations between SNP and microsatellite-derived estimates of genetic diversity. For example, previous work using 7 SNPs/indels and 14 microsatellites found that expected heterozygosity and allelic richness are positively correlated between the two types of markers in Atlantic salmon populations (Ryynanen *et al.*, 2007). On the contrary, SNP ( $n=1-46$ ) and microsatellite ( $n=10-27$ ) heterozygosities are not correlated for European and North American wolf populations (Vali *et al.*, 2008). Likewise, microsatellite-estimated diversity is different between *Bombus* bumble bee species, but similar when using RADseq loci (Lozier, 2014), thus diversity estimates from these two markers are not correlated.

In gopher tortoises, the rank order for allelic richness and observed heterozygosity was similar but not the same for immune gene SNPs and the full and partial microsatellite datasets, respectively. Similar observations have been made by other studies including those comparing SNPs and microsatellites in Atlantic salmon (Ryynanen *et al.*, 2007). Rank order may be skewed between the markers because microsatellites are poly-allelic while SNPs are di-allelic. In particular, for a microsatellite or SNP marker, there are  $n((n-1)/2)$  combinations that result in a heterozygote where  $n$  is the number of alleles. Thus, for a di-allelic marker, there is only one combination of alleles that results in a heterozygote, and for a microsatellite that has at least 5 alleles (i.e., the average allelic richness for our 10 microsatellites in the full microsatellite dataset), there are 10 combinations of alleles that are heterozygous. This could explain why observed heterozygosity was not correlated between SNPs and microsatellites for the partial microsatellite dataset.

Previous work with microsatellites showed that genetic variation was lower in western versus eastern *G. polyphemus* populations (Ennen *et al.*, 2010), and our results with the SNP and re-analysis of the full microsatellite datasets support this finding. For the partial microsatellite dataset, the FL and not LA

268 population had the lowest observed heterozygosity, but in the full microsatellite dataset, the LA population  
269 had the lowest observed heterozygosity. The full microsatellite dataset probably provides better estimates  
270 as 36 and 19 tortoises were analyzed for the LA and FL populations, respectively as compared to just four  
271 tortoises in the partial microsatellite dataset, therefore observed heterozygosity is likely lower in the LA  
272 than FL population. Because we only sampled a single western population (Fig. 1), it is not appropriate to  
273 generalize all western populations as genetically depauperate. Ultimately, additional sampling and immunome  
274 sequencing from other western *G. polyphemus* populations is warranted.

## 275 Genetic differentiation

276 We also observed strong correlations between SNP and microsatellite-derived genetic differentiation, al-  
277 beit the order of least to most differentiated comparisons varied. The same was observed for SNP- and  
278 microsatellite-derived  $F_{ST}$  estimates from four populations of western corn rootworms (Coates *et al.*, 2009).  
279 The incongruence in rank order may have occurred in both scenarios because of homoplasy issues with mi-  
280 crosatellites, where high mutation rates can cause repeat number to revert to a particular allele size, which  
281 can then inflate estimates of gene flow (Coates *et al.*, 2009).

## 282 Genetic admixture

283 Population admixture assessments had few inconsistencies between SNPs and microsatellites. Both PCAs  
284 suggested four clusters using either marker. We did observe differences in STRUCTURE admixture results with  
285 the optimum number of clusters being 2 for SNPs and 4 and 3 for the full and partial microsatellite datasets.  
286 Morin *et al.* (2012) compared 42 SNPs versus 22 microsatellites in bowhead whales and also found that the  
287 optimum number of clusters is different when using STRUCTURE. SNPs and microsatellites may have suggested  
288 different estimates of the optimum number of clusters because some of the SNPs may represent functional  
289 rather than neutral genetic variation like the microsatellites, with both types of markers differing to what  
290 extent they have been influenced by selection and/or genetic drift.

## 291 Experimental design considerations

292 So far, we have discussed how population genetic parameters estimated from immune gene SNPs mirror  
293 patterns estimated from microsatellite loci, but marker choice also depends on additional considerations such  
294 as cost, number of loci, computational issues with NGS generated SNPs, and neutral versus selective processes.  
295 First, although sequencing costs are decreasing, NGS techniques can be more expensive than microsatellites

on a per sample basis depending on availability of equipment. In particular, the NGS technique used in this paper, in-solution hybridization, requires synthesis of expensive RNA baits/probes, in the order of several thousand dollars (USD). Although tagged microsatellite primers are not trivial in cost, they are far cheaper than biotinylated RNA baits. Further, most genetics labs are not equipped for NGS workflows that require specialized equipment, so lab work must either be outsourced to commercial or non-commercial core facilities.

The number of loci required to adequately address the genetic question at hand is also an important consideration when choosing between SNPs and microsatellites and will vary depending on the question being asked. In general, simulations suggest many more SNPs are needed than microsatellite loci when trying to achieve similar statistical power or parameter estimates. For example, between 60–100 SNP loci are needed for accurate parentage assignment (Anderson & Garza, 2006), and empirical data from sockeye salmon suggest 80 SNPs have higher assignment success and are more accurate for parentage assignment than 11 microsatellites (Hauser *et al.*, 2011). Furthermore, a similar number of SNPs is needed for detecting low levels of divergence (i.e.,  $F_{ST} < 0.005$ ) (Morin *et al.*, 2009). Ryynanen *et al.* (2007) observed significant correlations between 7 SNPs/indels and 14 microsatellite loci when estimating  $F_{ST}$ . Our data subsampling results suggest at least 100 SNP loci are needed for correlating SNP and microsatellite-derived  $F_{ST}$ . For allelic richness and heterozygosities, our data suggest more than 800 SNP loci are needed to correlate with 10 microsatellite loci in *G. polyphemus*, but Ryynanen *et al.* (2007) only needed 7 SNP/indel loci to obtain similar correlations, possibly because they analyzed 21 populations. Acquiring data from a large number of SNPs is not a problem with NGS approaches, rather not all SNP loci are equally informative, and smaller SNP panels may occasionally perform well in comparison to much larger SNP arrays.

Computational issues with NGS are also not trivial, as our own NGS analysis relied on high performance computing resources and required many gigabytes of data storage. This does not include the time or expertise required to write code and scripts to analyze the gigabytes of raw data.

Neutral versus selective processes are also important to consider when deciding between SNPs and microsatellites. Markers such as microsatellites will be neutrally evolving while SNPs could represent both functional and neutral markers and be influenced by both neutral and adaptive processes. Our SNP data had very few SNPs that were putatively under selection (less than 1%), which is in line with previous NGS studies (e.g., Hohenlohe *et al.*, 2010; Lemay & Russello, 2015; Blanco-Bercial & Bucklin, 2016). This together with the observed correlations between SNPs and microsatellites suggests that most of our SNPs were effectively neutral. The gopher tortoise populations we surveyed appear to have small effective population sizes, likely less than 500 individuals per population, so perhaps the selection coefficients of many of the immune

327 gene SNPs were small enough (i.e., less than 0.1 %) that they behaved as effectively neutral loci.

## 328 Conclusion

329 As more and more population genetic studies are publishing NGS generated SNPs as opposed to mi-  
330 crosatellites, it would be useful to identify patterns between microsatellites and NGS derived SNPs and to  
331 appreciate the additional functional information commonly provided by SNPs. One apparent pattern is that  
332 high variation observed at microsatellites can translate into high SNP-estimates of genetic diversity (Ryyna-  
333 nen *et al.*, 2007) and vice versa. Further, genetic diversity estimated by allelic richness between microsatellites  
334 and SNPs may be a less stable metric than diversity estimated by observed and/or expected heterozygos-  
335 ity as more alleles are present in microsatellites than SNPs. This does not mean allelic richness should be  
336 ignored especially for conservation purposes because some traits including disease resistance are associated  
337 with particular alleles (e.g., Langefors *et al.*, 2001), which is not accounted for by heterozygosity. Another  
338 important pattern that may be observed between microsatellites and SNP studies is presence/absence of  
339 genetic structure, with any potential inconsistencies resulting from different evolutionary forces acting on the  
340 markers. The addition of adaptive processes acting on SNPs can result in similar but disparate structure  
341 patterns between the two marker types. Finally, even SNPs that are putatively influenced by selection may  
342 behave as effectively neutral loci when effective population sizes are small, thus we recommend researchers  
343 consider when comparing population genetic results derived from potentially functional and neutral markers  
344 in small populations such as those of threatened and endangered species.

## 345 Acknowledgements

346 This material is based upon work that is supported by the National Institute of Food and Agriculture, U.S.  
347 Department of Agriculture, McIntire Stennis project LAB04066 and LAB94169. The Lucius Gilbert Foun-  
348 dation provided support for sequencing and for J.P.E. We are grateful to Richard Carmouche of Pennington  
349 Biomedical Research Center's Genomic Core Facility for performing next-generation sequencing laboratory  
350 work. This project/work used genomics core facilities that are supported in part by COBRE (NIH 8 P20  
351 GM103528) and NORC (NIH 2P30DK072476) center grants from the National Institutes of Health. We  
352 appreciate the access we had to the LSU High Performance Computing resources, which we used to analyze  
353 next-generation sequencing data.

## References

- Allendorf FW, Hohenlohe PA, Luikart G (2010) Genomics and the future of conservation genetics. *Nature Reviews Genetics*, **11**, 697–709.
- Anderson EC, Garza JC (2006) The power of single-nucleotide polymorphisms for large-scale parentage inference. *Genetics*, **172**, 2567–2582.
- Benjamini Y, Hochberg Y (1995) Controlling the false discovery rate: A practical and powerful approach to multiple testing. *Journal of the Royal Statistical Society. Series B (Methodological)*, **57**, 289–300.
- Bernatchez L, Landry C (2003) MHC studies in nonmodel vertebrates: what have we learned about natural selection in 15 years? *Journal of Evolutionary Biology*, **16**, 363–377.
- Blanco-Bercial L, Bucklin A (2016) New view of population genetics of zooplankton: RAD-seq analysis reveals population structure of the North Atlantic planktonic copepod *Centropages typicus*. *Molecular Ecology*, **25**, 1566–80.
- Bolger AM, Lohse M, Usadel B (2014) TRIMMOMATIC: a flexible trimmer for Illumina sequence data. *Bioinformatics*, p. btu170.
- Browning SR, Browning BL (2007) Rapid and accurate haplotype phasing and missing-data inference for whole-genome association studies by use of localized haplotype clustering. *American Journal of Human Genetics*, **81**, 1084–97.
- Clostio RW, Martinez AM, LeBlanc KE, Anthony NM (2012) Population genetic structure of a threatened tortoise across the south-eastern United States: implications for conservation management. *Animal Conservation*, **15**, 613–625.
- Coates BS, Sumerford DV, Miller NJ, *et al.* (2009) Comparative performance of single nucleotide polymorphism and microsatellite markers for population genetic analysis. *Journal of Heredity*, **100**, 556–564.
- Danecek P, Auton A, Abecasis G, *et al.* (2011) The Variant Call Format and VCFtools. *Bioinformatics*, **27**, 2156–8.
- De Wit P, Pespeni MH, Ladner JT, *et al.* (2012) The simple fool’s guide to population genomics via RNA-Seq: an introduction to high-throughput sequencing data analysis. *Molecular Ecology Resources*, **12**, 1058–67.
- DeFaveri J, Viitaniemi H, Leder E, Meril   J (2013) Characterizing genic and nongenic molecular markers: comparison of microsatellites and SNPs. *Molecular Ecology Resources*, **13**, 377–392.
- Do C, Waples RS, Peel D, Macbeth G, Tillett BJ, Ovenden JR (2014) NeEstimator v2: re-implementation of software for the estimation of contemporary effective population size ( $N_e$ ) from genetic data. *Molecular Ecology Resources*, **14**, 209–214.
- Earl DA, vonHoldt BM (2012) STRUCTURE HARVESTER: a website and program for visualizing STRUCTURE output and implementing the Evanno method. *Conservation Genetics Resources*, **4**, 359–361.
- Elbers JP, Taylor SS (2015) GO2TR: a gene ontology-based workflow to generate target regions for target enrichment experiments. *Conservation Genetics Resources*, **7**, 851–857.
- Enge K, Berish J, Bolt R, Dziergowski A, Musinsky H (2006) Biological status report gopher tortoise. Report, Florida Fish and Wildlife Conservation Commission.
- Ennen JR, Kreiser BR, Qualls CP (2010) Low genetic diversity in several gopher tortoise (*Gopherus polyphemus*) populations in the Desoto National Forest, Mississippi. *Herpetologica*, **66**, 31–38.

393 Excoffier L, Lischer HE (2010) Arlequin suite ver 3.5: a new series of programs to perform population genetics  
394 analyses under Linux and Windows. *Molecular Ecology Resources*, **10**, 564–7.

395 Foll M, Gaggiotti O (2008) A genome-scan method to identify selected loci appropriate for both dominant  
396 and codominant markers: a Bayesian perspective. *Genetics*, **180**, 977–993.

397 Frankham R, Ballou JD, Briscoe DA (2010) *Introduction to conservation genetics*. Cambridge University  
398 Press, Cambridge, 2nd edn..

399 Garke C, Ytournal F, Bedhom B, *et al.* (2012) Comparison of SNPs and microsatellites for assessing the  
400 genetic structure of chicken populations. *Animal Genetics*, **43**, 419–428.

401 Glover KA, Hansen MM, Lien S, Als TD, Hoyheim B, Skaala O (2010) A comparison of SNP and STR loci  
402 for delineating population structure and performing individual genetic assignment. *BMC Genetics*, **11**,  
403 1–12.

404 Goudet J (2005) HIERFSTAT, a package for R to compute and test hierarchical F-statistics. *Molecular*  
405 *Ecology Notes*, **5**, 184–186.

406 Gupta P, Roy J, Prasad M (2001) Single nucleotide polymorphisms SNPs: a new paradigm in molecular  
407 marker technology and DNA polymorphism detection with emphasis on their use in plants. *Current*  
408 *Science*, **80**, 524–535.

409 Hauser L, Baird M, Hilborn RAY, Seeb LW, Seeb JE (2011) An empirical comparison of SNPs and microsatel-  
410 lites for parentage and kinship assignment in a wild sockeye salmon (*Oncorhynchus nerka*) population.  
411 *Molecular Ecology Resources*, **11**, 150–161.

412 Hohenlohe PA, Bassham S, Etter PD, Stiffler N, Johnson EA, Cresko WA (2010) Population genomics of  
413 parallel adaptation in threespine stickleback using sequenced RAD tags. *PLoS Genetics*, **6**, e1000862.

414 Hubisz MJ, Falush D, Stephens M, Pritchard JK (2009) Inferring weak population structure with the assis-  
415 tance of sample group information. *Molecular Ecology Resources*, **9**, 1322–32.

416 Jeffries DL, Copp GH, Lawson Handley L, Olsen KH, Sayer CD, Hanfling B (2016) Comparing RADseq and  
417 microsatellites to infer complex phylogeographic patterns, an empirical perspective in the Crucian carp,  
418 *Carassius carassius*, L. *Molecular Ecology*, p. in press.

419 Kopelman NM, Mayzel J, Jakobsson M, Rosenberg NA, Mayrose I (2015) CLUMPAK: a program for identify-  
420 ing clustering modes and packaging population structure inferences across k. *Molecular Ecology Resources*,  
421 **15**, 1179–91.

422 Langefors A, Lohm J, Grahn M, Andersen O, von Schantz T (2001) Association between major histocompat-  
423 ibility complex class iiB alleles and resistance to *Aeromonas salmonicida* in atlantic salmon. *Proceedings of*  
424 *the Royal Society of London B*, **268**, 479–485.

425 Lemay MA, Russello MA (2015) Genetic evidence for ecological divergence in kokanee salmon. *Molecular*  
426 *Ecology*, **24**, 798–811.

427 Li H (2013) Aligning sequence reads, clone sequences and assembly contigs with BWA-MEM. *arXiv*,  
428 **1303.3997**.

429 Li H, Durbin R (2009) Fast and accurate short read alignment with Burrows-Wheeler transform. *Bioinfor-*  
430 *matics*, **25**, 1754–60.

431 Li H, Handsaker B, Wysoker A, *et al.* (2009) The Sequence Alignment/Map format and SAMtools. *Bioin-*  
432 *formatics*, **25**, 2078–9.

433 Liao Y, Smyth GK, Shi W (2014) featureCounts: an efficient general purpose program for assigning sequence  
434 reads to genomic features. *Bioinformatics*, **30**, 923–30.

435 Lischer H, Excoffier L (2012) PGDSpider: an automated data conversion tool for connecting population  
436 genetics and genomics programs. *Bioinformatics*, **28**, 298–299.

437 Lozier JD (2014) Revisiting comparisons of genetic diversity in stable and declining species: assessing genome-  
438 wide polymorphism in North American bumble bees using RAD sequencing. *Molecular Ecology*, **23**, 788–  
439 801.

440 Lunter G, Goodson M (2011) STAMPY: a statistical algorithm for sensitive and fast mapping of Illumina  
441 sequence reads. *Genome Research*, **21**, 936–9.

442 McKenna A, Hanna M, Banks E, *et al.* (2010) The Genome Analysis Toolkit: a MapReduce framework for  
443 analyzing next-generation DNA sequencing data. *Genome Research*, **20**, 1297–1303.

444 Miller HC, Miller KA, Daugherty CH (2008) Reduced MHC variation in a threatened tuatara species. *Animal*  
445 *Conservation*, **11**, 206–214.

446 Morin PA, Archer FI, Pease VL, *et al.* (2012) An empirical comparison of SNPs and microsatellites for  
447 population structure, assignment, and demographic analyses of bowhead whale populations. *Endangered*  
448 *Species Research*, **19**, 129–147.

449 Morin PA, Martien KK, Taylor BL (2009) Assessing statistical power of SNPs for population structure and  
450 conservation studies. *Molecular Ecology Resources*, **9**, 66–73.

451 Moritz C (1994) Applications of mitochondrial DNA analysis in conservation: a critical review. *Molecular*  
452 *Ecology*, **3**, 401–411.

453 Narum SR, Banks M, Beacham TD, *et al.* (2008) Differentiating salmon populations at broad and fine  
454 geographical scales with microsatellites and single nucleotide polymorphisms. *Molecular Ecology*, **17**, 3464–  
455 3477.

456 Nomura T (2008) Estimation of effective number of breeders from molecular coancestry of single cohort  
457 sample. *Evolutionary Applications*, **1**, 462–474.

458 Ortutay C, Vihinen M (2006) Immunome: a reference set of genes and proteins for systems biology of the  
459 human immune system. *Cellular Immunology*, **244**, 87–89.

460 Pritchard JK, Stephens M, Donnelly P (2000) Inference of population structure using multilocus genotype  
461 data. *Genetics*, **155**, 945–959.

462 R Core Team (2015) *R: A Language and Environment for Statistical Computing*. R Foundation for Statistical  
463 Computing, Vienna, Austria.

464 Ryyanen HJ, Tonteri A, Vasemagi A, Primmer CR (2007) A comparison of biallelic markers and microsatel-  
465 lites for the estimation of population and conservation genetic parameters in Atlantic salmon (*Salmo salar*).  
466 *Journal of Heredity*, **98**, 692–704.

467 Shaffer HB, Minx P, Warren DE, *et al.* (2013) The western painted turtle genome, a model for the evolution  
468 of extreme physiological adaptations in a slowly evolving lineage. *Genome Biology*, **14**, R28.

469 Sommer S (2005) The importance of immune gene variability (MHC) in evolutionary ecology and conservation.  
470 *Frontiers in Zoology*, **2**, 16–16.

471 Taylor SS, Jenkins DA, Arcese P (2012) Loss of MHC and neutral variation in Peary caribou: genetic drift  
472 is not mitigated by balancing selection or exacerbated by MHC allele distributions. *PLoS One*, **7**, e36748.



473 Vali U, Einarsson A, Waits L, Ellegren H (2008) To what extent do microsatellite markers reflect genome-wide  
 474 genetic diversity in natural populations? *Molecular Ecology*, **17**, 3808–3817.

475 Waples RS, Do C (2008) LDNE: a program for estimating effective population size from data on linkage  
 476 disequilibrium. *Molecular Ecology Resources*, **8**, 753–756.

477 Weber DS, Stewart BS, Schienman J, Lehman N (2004) Major histocompatibility complex variation at three  
 478 class II loci in the northern elephant seal. *Molecular Ecology*, **13**, 711–718.

479 Wright S (1931) Evolution in mendelian populations. *Genetics*, **16**, 97–159.

480 Zhdanova OL, Pudovkin AI (2008) Nb\_HetEx: a program to estimate the effective number of breeders.  
 481 *Journal of Heredity*, **99**, 694–695.

## 482 Data Accessibility

483 Raw sequencing data are available from the Sequence Read Archive (accession: SRP061247). BAM and VCF  
 484 files are available from Dryad repository (doi: 10.5061/dryad.40c7c). Detailed analytical methods and scripts  
 485 to create Tables and Figures are available from [https://github.com/jelber2/immunome\\_2014](https://github.com/jelber2/immunome_2014).

## 486 Author Contributions

487 J.P.E. designed the study and performed SNP analyses. R.W.C. performed microsatellite analyses. J.P.E.  
 488 and S.S.T. wrote the paper.

## 489 Supporting Information

490 Additional Supporting Information may be found in the online version of this article:

491 **Table S1** Sequencing metrics for *Gopherus polyphemus* samples. Percent UR for percent of total reads that  
 492 were unique, Percent URA for percent of unique reads that were alignable, Mean coverage for mean number  
 493 of reads across the target region, Percent 20x for percent of bases in target region with greater than 20x  
 494 coverage, No. genes for number of genes, and No. exons for number of exons.

495 **Table S2** All genes with di-allelic, polymorphic SNPs from 16 *Gopherus polyphemus* samples.

496 **Fig. S1** Coverage plots for first eight *Gopherus polyphemus* samples showing number of sequencing reads at  
 497 or above specified proportions. A value at 100 Depth and 0.5 fraction means 50 percent of bases were at or  
 498 above 100X coverage.

499 **Fig. S2** Coverage plots for last eight *Gopherus polyphemus* samples showing number of sequencing reads at

500 or above specified proportions.

501 **Fig. S3** STRUCTURE plot for 16 *Gopherus polyphemus* sequenced at 17,901 immune gene SNPs with optimum  
502 number of clusters  $K = 2$  determined by STRUCTURE HARVESTER.

503 **Fig. S4** STRUCTURE plot for the full microsatellite dataset (101 *Gopherus polyphemus* genotyped at 10 mi-  
504 crosatellite loci) with optimum number of clusters  $K = 4$  determined by STRUCTURE HARVESTER.

505 **Fig. S5** STRUCTURE plot for the partial microsatellite dataset (16 *Gopherus polyphemus* genotyped at 10  
506 microsatellite loci) with optimum number of clusters  $K = 3$  determined by STRUCTURE HARVESTER.

507 **Fig. S6** Subsampling analysis showing how many randomly sampled SNP loci out of the total of 17,901 are  
508 needed in comparison to the full microsatellite dataset (101 *Gopherus polyphemus* genotyped at 10 microsatel-  
509 lite loci) for Pearson's  $r$  correlation coefficient to be significant at 0.05 level (dotted line) for (A) observed  
510 heterozygosity; (B) expected heterozygosity; and (C)  $F_{ST}$ . There were 10 simulations for each size class of  
511 SNPs.  $H_O$  for observed heterozygosity,  $H_E$  for expected heterozygosity.

512 **Fig. S7** Subsampling analysis showing how many randomly sampled SNP loci out of the total of 17,901  
513 are needed in comparison to the partial microsatellite dataset (16 *Gopherus polyphemus* genotyped at 10 mi-  
514 crosatellite loci) for Pearson's  $r$  correlation coefficient to be significant at 0.05 level (dotted line) for (A) allelic  
515 richness; (B) expected heterozygosity; and (C)  $F_{ST}$ . There were 10 simulations for each size class of SNPs.  
516  $A_R$  for allelic richness,  $H_E$  for expected heterozygosity.

517 **Fig. S8** Effective population sizes per generation ( $N_e$ ) along with 95 % confidence intervals for *Gopherus*  
518 *polyphemus* samples estimated with the program NeEstimator using (A) the full microsatellite dataset (101  
519 *G. polyphemus* genotyped at 10 microsatellite loci) or (B) the SNP dataset (16 *G. polyphemus* sequenced at  
520 17,901 immune gene SNPs). Dots that are on the top of the graph represent  $N_e$  estimates of infinity, and  
521 lines that extend to the top of the graph represent upper 95 % confidence limits of infinity. LD for linkage  
522 disequilibrium method of Waples & Do (2008), HET for heterozygote-excess method of Zhdanova & Pudovkin  
523 (2008), and MOL for the molecular coancestry method of Nomura (2008). Note that the HET and MOL  
524 methods estimate the effective number of breeders per year ( $N_b$ ), which were converted to  $N_e$  by multiplying  
525  $N_b$  by the generation time of 31 years for *G. polyphemus* (Enge et al. 2006).

526

## 527 Tables and Figures

528 **Table 1** Comparisons of full (101 individuals) and partial (16 individuals) microsatellite datasets with SNP  
 529 dataset (16 individuals) for *Gopherus polyphemus*. Values with decimals represent mean population genetic  
 530 parameter values. AR for allelic richness, Ho for observed heterozygosity, HE for expected heterozygosity,  
 531 No. pops for number of optimum populations determined with STRUCTURE HARVESTER for STRUCTURE or  
 532 visually for PCA.

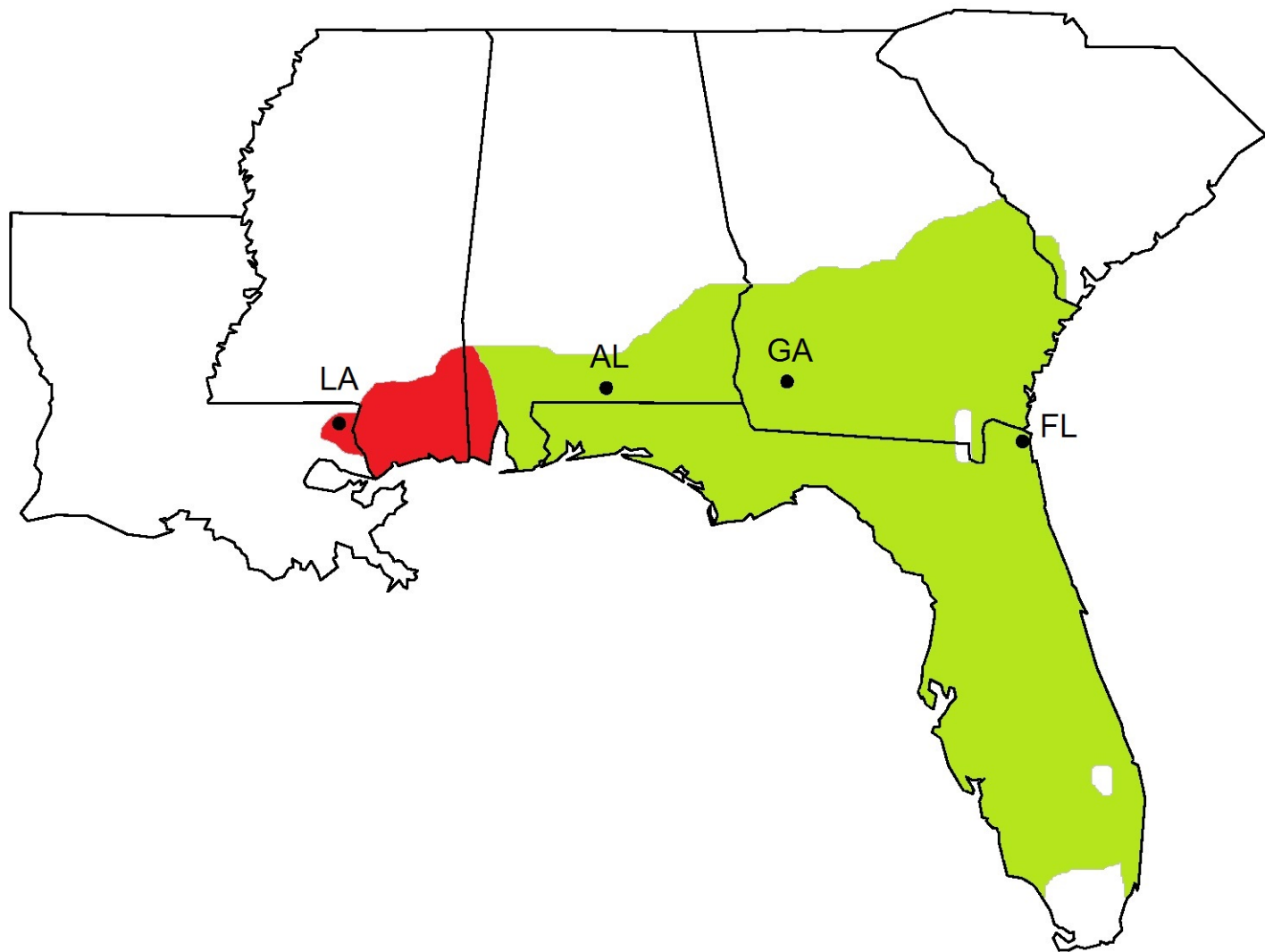
Variable	SNP dataset	Full Microsatellite Dataset	Partial Microsatellite Dataset
AR	1.541	5.487	2.900
Correlation with SNPs		not significant	not significant
Ho	0.267	0.495	0.469
Correlation with SNPs		significant	not significant
HE	0.228	0.543	0.531
Correlation with SNPs		significant	significant
FST	0.282	0.336	0.320
Correlation with SNPs		significant	significant
No. pops STRUCTURE	2	4	3
No. pops PCA	4	4	4

533

534 **Table 2** Histocompatibility and Toll-like Receptor Loci with di-allelic, polymorphic SNPs in the *Gopherus*  
535 *polyphemus* SNP dataset (16 *G. polyphemus* sequenced at 17,901 immune gene SNPs).

Histocompatibility Loci
CD74 molecule, major histocompatibility complex, class II invariant chain
Class I histocompatibility antigen, F10 alpha chain-like
Class II histocompatibility antigen, M alpha chain
Class II, major histocompatibility complex, transactivator
DLA class II histocompatibility antigen, DR-1 beta chain-like
H-2 class II histocompatibility antigen, A-R alpha chain-like
H-2 class II histocompatibility antigen, E-S beta chain-like
HLA class II histocompatibility antigen, DP alpha 1 chain-like
HLA class II histocompatibility antigen, DR alpha chain-like
HLA class II histocompatibility antigen, DR beta 5 chain-like
HLA class II histocompatibility antigen, DRB1-15 beta chain-like
Major histocompatibility complex class I-related gene protein-like
Rano class II histocompatibility antigen, A beta chain-like
Toll-like Receptor Loci
Toll-like Receptor 13
Toll-like Receptor 2
Toll-like Receptor 7
Toll-like Receptor 8
Toll-like Receptor adaptor molecule 1
Toll-like Receptor adaptor molecule 2

536



537

538 **Fig. 1** *Gopherus polyphemus* range map and sampling sites used in this study. Range of western *G. polyphe-*  
 539 *mus* populations darkly shaded on the left with eastern populations lightly shaded on the right. LA for  
 540 Florida Gas Pipeline, Washington Parish, Louisiana, USA (latitude, longitude, sample size for full microsatel-  
 541 lite dataset = 30.78, -90.00;  $N = 36$ ). AL for Solon Dixon, Andalusia, Alabama, USA (31.16, -86.70;  $N =$   
 542 20). GG for Jones Ecological Research Center, Georgia, USA. (31.23, -84.47;  $N = 26$ ). FL for Private Site,  
 543 Nassau County, Florida, USA (30.59, -81.56;  $N = 19$ ).  
 544

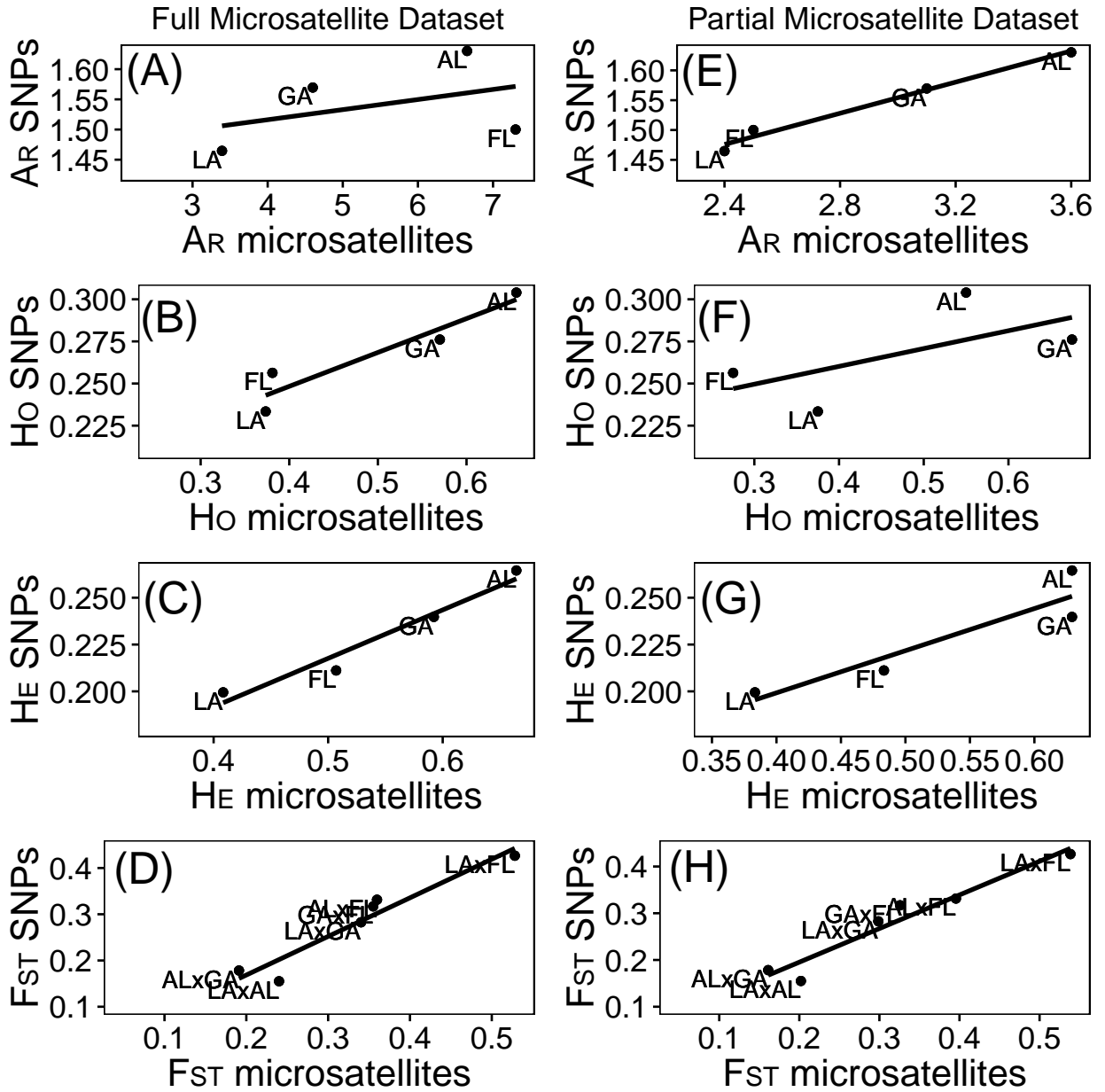


**Fig. 2** Correlations between 10 microsatellites and 17,901 immune gene SNPs for *Gopherus polyphemus* samples. Left column for full microsatellite dataset (101 *G. polyphemus* genotyped at 10 microsatellites) for (A) allelic richness, Pearson's  $r = 0.411$ ,  $P = 0.294$ ; (B) observed heterozygosity, Pearson's  $r = 0.945$ ,  $P = 0.028$ ; (C) expected heterozygosity, Pearson's  $r = 0.976$ ,  $P = 0.012$ ; and (D) FST, Pearson's  $r = 0.96$ ,  $P = 0.001$ . Right column for partial microsatellite dataset (16 *G. polyphemus* genotyped at 10 microsatellites) for (E) allelic richness, Pearson's  $r = 0.992$ ,  $P = 0.004$ ; (F) observed heterozygosity, Pearson's  $r = 0.63$ ,  $P = 0.185$ ; (G) expected heterozygosity, Pearson's  $r = 0.924$ ,  $P = 0.038$ ; and (H) FST, Pearson's  $r = 0.968$ ,  $P = 0.001$ . AR for allelic richness, Ho for observed heterozygosity, He for expected heterozygosity.

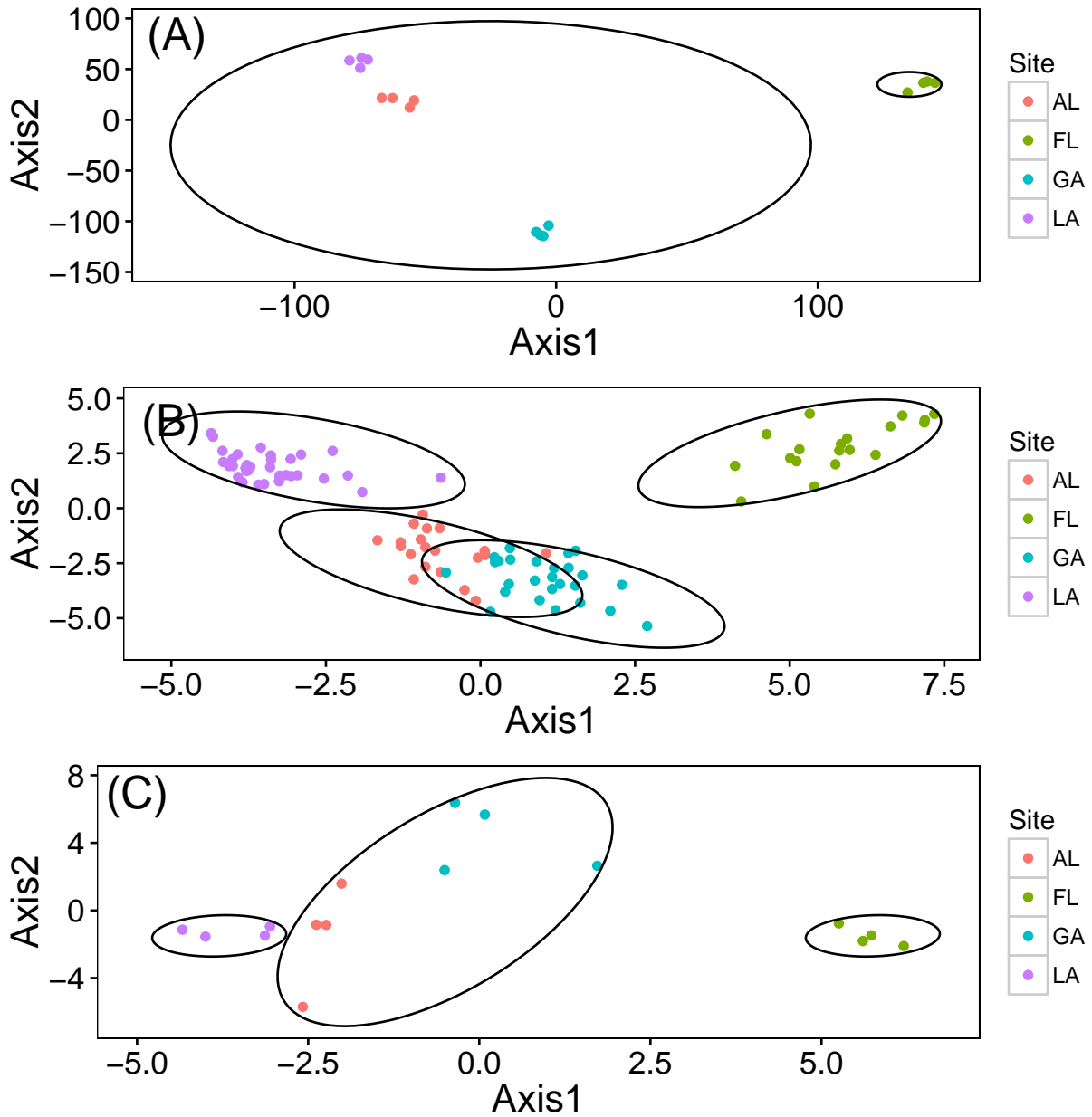


**Fig. 3** Principle component analysis for *Gopherus polyphemus* datasets: (A) the SNP dataset (16 *G. polyphemus* sequenced at 17,901 immune gene SNPs); (B) full microsatellite dataset (101 *G. polyphemus* genotyped at 10 microsatellites); and (C) partial microsatellite dataset (16 *G. polyphemus* genotyped at 10 microsatellites). Circles indicate optimum clusters identified using STRUCTURE and STRUCTURE HARVESTER.